Electrical TCAD Simulation of STT-MRAMs

Hanane C. Saifi
Aix-Marseille Univ
CNRS, IM2NP
Marseille, France
hanane-chems.saifi@etu.univ-amu.fr

Jérémy Postel-Pellerin
Aix-Marseille Univ
CNRS, IM2NP
Marseille, France
jeremy.postel-pellerin@univ-amu.fr

Nicole Yazigy
Aix-Marseille Univ
CNRS, IM2NP
Marseille, France
nicole.yazigy@univ-amu.fr

Noémie Couzi
Aix-Marseille Univ
CNRS, IM2NP
Marseille, France
noemie.couzi@univ-amu.fr

Vincenzo Della Marca
Aix-Marseille Univ
CNRS, IM2NP
Marseille, France
vincenzo.della-marca@univ-amu.fr

Pierre Canet
Aix-Marseille Univ
CNRS, IM2NP
Marseille, France
pierre.canet@univ-amu.fr

Nuno Caçoilo
SPINTEC, University Grenoble Alpes, CNRS, CEA-SPINTEC, CEA
Grenoble, France
nuno.cacoilo@cea.fr

Grégory Di Pendina
SPINTEC, University Grenoble Alpes, CNRS, CEA-SPINTEC, CEA
Grenoble, France
gregory.dipendina@cea.fr

Ricardo C. Sousa
SPINTEC, University Grenoble Alpes, CNRS, CEA-SPINTEC, CEA
Grenoble, France
ricardo.sousa@cea.fr

2024 International Conference on Simulation of Semiconductor Processes and Devices (SISPAD) | 979-8-3315-1635-2/24/$31.00 ©2024 IEEE | DOI: 10.1109/SISPAD62626.2024.10733096

***Abstract*—In this paper, we propose to develop a full TCAD simulation, using a commercial tool (Sentaurus), of an STT-MRAM device to better understand its electrical behavior. To our knowledge, it is the first time that a simulated I-V hysteresis loop is calibrated on experimental data. The impact of several key parameters is presented, and the obtained values are in good agreement with the ones found in literature. This calibrated TCAD simulation can then be used to study the variability of the switching voltages, the temperature dependence, or the impact of process variations.**

Keywords— STT-MRAM, Magnetic Tunnel Junction MTJ, TCAD simulation, Landau–Lifshitz–Gilbert

I. Introduction

A promising non-volatile memory known as Spin-Transfer Torque Magnetic Random-Access Memory (STT-MRAM) combines a fast writing operation with a high density and significant endurance (up to 10^{13} cycles) [1, 2]. Magnetization direction is the form in which the data in Magnetic Tunnel Junctions (MTJ) is coded and its read/write latency is controlled by the stochastic nature of the reversal, device size, and current flowing through the layers [2].

The MTJs are composed of a CoFeB/MgO/CoFeB stack, where the MgO insulator layer serves as a tunnel barrier layer. Programming the cell from the Anti-Parallel (AP) to the Parallel (P) state and vice-versa is performed by forcing a spin-polarized current through the device as illustrated in Fig. 1. An important characteristic of the MTJ is the Tunnel Magnetoresistance Ratio (TMR) defined as $(R_{AP}–R_P)/R_P$, where R_{AP} and R_P are the resistances of AP and P states respectively [3]. To perform the quasi-static current versus voltage (I-V) loop, as shown in Fig. 1, the bias voltage is applied to the top electrode of the MTJ, with a resistance-area product R.A~12Ω·μm^2, a TMR~100%, and a diameter~100nm, while grounding the bottom electrode and measuring the top electrode current. A voltage ramp is applied to write the cell with a positive bias to switch the cell to the P state and a negative bias to switch it to the AP state. The reading voltage (V_R=+100mV) is chosen to determine the cell state, without modifications, and to extract the corresponding resistance value.

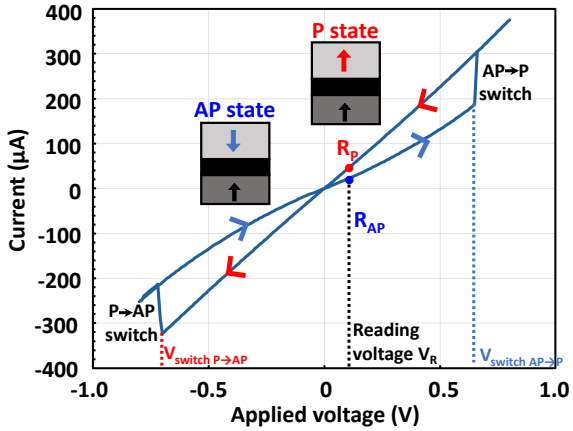

Fig. 1. Quasi-static experimental I-V hysteresis loop of state transitions of the Magnetic Tunnel Junction.

In previous studies, we experimentally demonstrated the stochastic behavior of the switching phenomenon in STT-MRAM [4] and the impact of an infrared laser attack on the MTJ [5,6]. A nuanced understanding of the functioning of such a device is necessary to explain the observed phenomena and improve the nanofabrication process of the whole stack for better performance and/or robustness. To this goal, a Technology Computer Aided-Design (TCAD) approach, especially using Sentaurus from Synopsis®, can be very useful but only a few previous studies have focused on this subject. Indeed, a first study was proposed by F.O. Heinz et al. [7] implementing the Landau–Lifshitz–Gilbert (LLG) equations [8] in Sentaurus, showing the capacity to reverse the magnetization in the Free Layer. Some studies have used other tools [9, 10, 11] but, to our knowledge, none of them proposed the simulation of the whole MTJ stack and/or the electrical simulation of the I-V hysteresis loop. In this work we propose to develop the main calibration steps of the electrical simulation to achieve the full I-V hysteresis loop and the variability estimation of the switching voltages of our device. This work also sets the path for a thermal analysis of the MTJ.

II. TCAD Simulation of the MTJ Stack

A. Bi-dimensional definition of the MTJ stack

The first step for the TCAD simulation is to reproduce in 2D the whole MTJ stack (with a width of 100nm) using Sentaurus Structure Editor. Fig. 2 shows the simulated structure (left) and a High-Resolution Transmission Electron Microscopy (HRTEM) of the whole stack used in our study (right). For improved accuracy, a specific meshing is performed in the 3 main layers (CoFeB/MgO/CoFeB) of the structure.

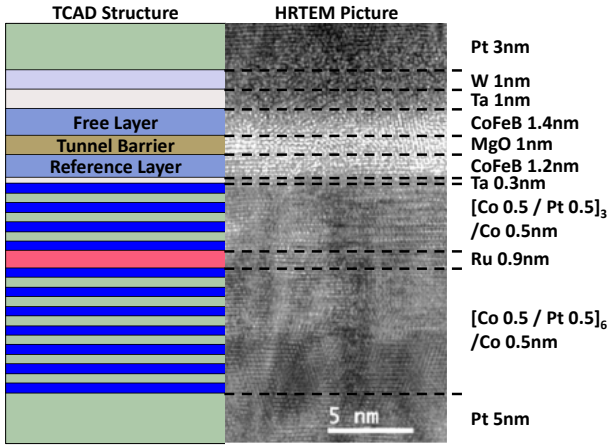

Fig. 2. Simulated (left) and HRTEM picture (right) of the p-MTJ [12].

Note that some materials such as CoFeB, MgO and Ru do not exist natively in Sentaurus, so specific parameters files have been created to define their main constants (permittivity, conductivity, thermal conductivity, ...).

B. Electrical simulation of the MTJ at 298K

We have then implemented in Sentaurus Device the required magnetic and tunneling models (Thermal Fluctuations, Macro Spin, Direct Tunneling) as described in [13]. At 298K, we used the default values for: the Stoner–Wohlfarth switching field H_k, the effective magnetization M_{eff}, the effective mass in ferromagnet m_{FM}, the density-of-states mass parallel to the interface m_{dos}, the Fermi energy in ferromagnet relative to conduction band E_F, the energy barrier between the ferromagnet and the barrier U_B, and the Gilbert damping coefficient α, according to [13]. For the three remaining parameters: the effective mass in barrier m_{ox} and the energy splitting between spin-up and spin-down electrons in ferromagnet D_{spin}, both related to the R_{AP} and RP values, and the saturation magnetization of the ferromagnetic material M_S related to the switching voltages, several values can be found in literature [11, 13, 14]. Fig. 3 presents the impact of m_{ox} and D_{spin} on the resistance values extracted at V_R=100mV, showing a weak effect on R_P but a large variation of R_{AP}. The experimental resistance targets are fixed by the values extracted from Fig. 1.

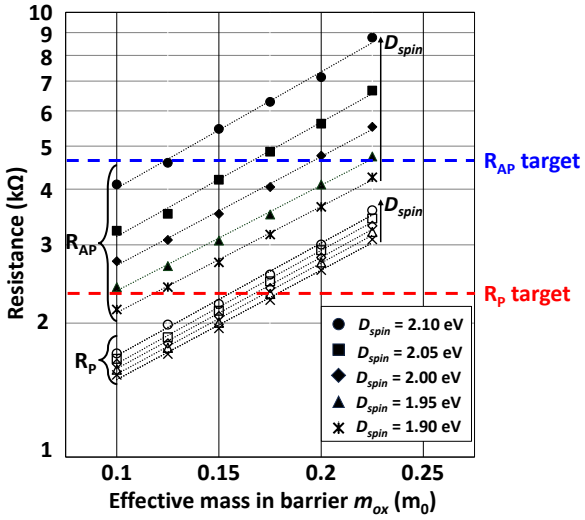

Fig. 3. Impact of m_{ox} and D_{spin} parameters on the R_P and R_{AP} values.

We fixed m_{ox}=0.16m_0 which is coherent with [13] and D_{spin}=2.06 eV in the range [1.98 eV; 2.15 eV] from [11] and [13]. In the LLG equation, thermal fluctuations create stochastic fields, impacting magnetization dynamics under the Macrospin approximation. Despite consistent saturation magnetization (M_S), switching voltages vary across realizations. Fig. 4 depicts this variability, showing minimum, mean, and maximum switching voltages from 30 simulations per M_S value, with M_S varying from 0.8x10^{6}A/m (from [13]) to 1.3 x10^{6}A/m (from [14]).

The simulations are then carried out with M_S=1.2x10^{6}A/m, which is coherent with values from [9, 14]. Fig. 5 shows the comparison between an experimental I-V hysteresis loop (solid black line) and 100 realizations in simulation (dotted grey lines) with a very good agreement as well for R_{AP} and R_P values as for switching voltages.

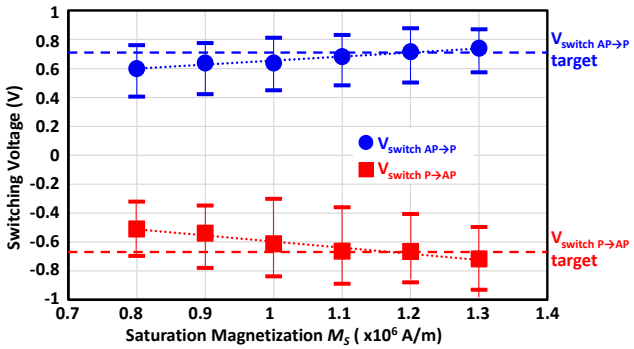

Fig. 4. Impact of M_S parameter on the switching voltages.

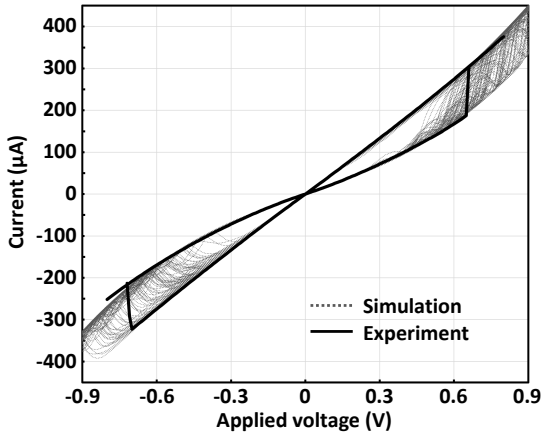

Fig. 5. Comparison between an experimental I-V hysteresis loop and 100 realizations in simulation at 298K.

III. Simulation of the Thermal Effects

After calibrating the electrical simulation at room temperature (T=298K), we want to reproduce the electrical behavior of our device at higher temperatures, using previous experimental data from [6] showing a decrease in the R_{AP} value and a slight increase in the R_P value, between T=298K and T=378K. We will focus on the thermal simulation of these resistance values and the associated TMR value.

A. Impact of temperature on the model parameters

The first step to consider temperature in simulation is to implement the thermal conductivity of the different materials of the MTJ stack (Co, CoFeB, MgO, ...) [15]. Concerning the electrical model by itself, among all the parameters presented in section II.B, most are almost independent on temperature and will remain constant over the considered temperature range, such as M_{eff}, m_{FM}, m_{dos}, E_F, D_{spin}, α [16], H_k (only varying in $\sqrt{T}$ [17]). According to the Bloch law (Equation 1) [18, 19, 20, 21], the M_S parameter varies with temperature T as):

$$M_S(T) = M_S(0).\left(1 - \frac{T}{T_C}\right)^{3/2} \quad (1)$$

where T_C is the Curie temperature of CoFeB (1150K in [21])

The change in M_S can also lead to more fluctuations of the magnetization direction, i.e. larger variability from the equilibrium direction, resulting in a decrease of spin polarization. Perhaps we can just summarize this by saying that in a first approach changes in M_S were not considered due to the limited temperature range studied. We have chosen to consider the two remaining parameters, U_B and m_{ox}, which have the larger thermal variation [22, 23, 24] and impact on the resistance values. We first manually modified these two parameters to fit our experimental data between 298K and 378K each 20K. Resulting parameters values (marks) are presented in Fig. 6. Fitting equations (dotted lines) have then been established to match these values and predict the behavior at any temperature. According to [18, 23, 25], the energy barrier U_B can be modeled using Equation (2):

$$U_B(T) = U_B(0).\left(1 - \frac{T}{T_C}\right)^n \quad (2)$$

The fit was obtained using $U_B(0) = 3.619eV, T_C = 1150K$ as in [21] and $n = 1.57$, coherent with values from [25]. According to [24], the effective mass in barrier m_{ox} can be approximated using a quadratic polynomial although a linear dependence might be enough within the limited temperature range considered, as presented in Equation (3):

$$m_{ox}(T) = a + b.T + c.T^2 \quad (3)$$

The fit was obtained using $a = 4 \times 10^{-2}.m_0, b = -7.3 \times 10^{-5}.m_0.K^{-1}, and\ c = 1.6 \times 10^{-6}.m_0.K^{-2}$.

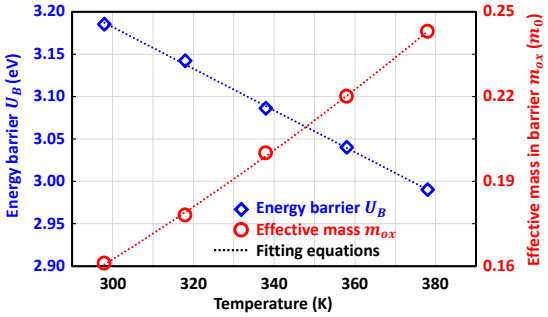

Fig. 6. Impact of temperature on U_B and m_{ox} parameters. Manually fitted values correspond to marks and fitting equations correspond to dotted lines.

B. Simulation results including temperature: Resistance values and TMR

We next used the 2 fitting equations for U_B and m_{ox} to simulate the R_P and R_{AP} values (crosses), presented in Fig. 7 and compared to experimental values (marks) from [6]. As previously mentioned in section II.B, the thermal fluctuations in the LLG equation implemented in our tool imply variability in the simulated values. Each resistance value represents the average from 10 simulations. We can notice a very good agreement between measurements and simulations, validating our approach. The TMR ratio is also plotted in Fig. 8, demonstrating excellent agreement between experimental values from [6] (marks) and simulations (crosses).

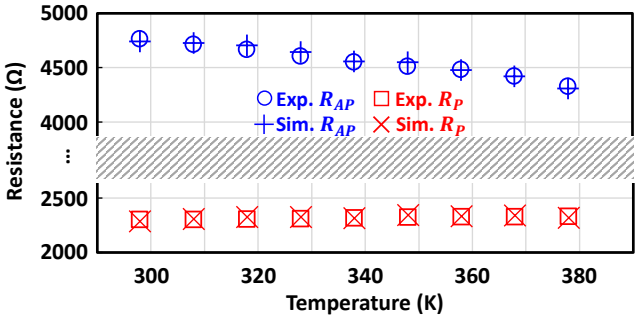

Fig. 7. Comparison between simulated (crosses) and experimental, from [6] (marks), R_P and R_{AP} values, between 298K and 378K.

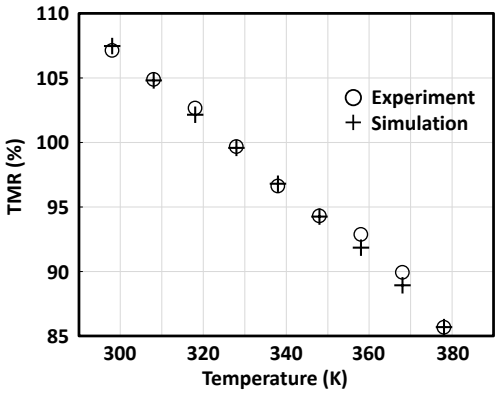

Fig. 8. Comparison between simulated (crosses) and experimental, from [6] (marks), TMR ratios, between 298K and 378K.

IV. Conclusion

The TCAD simulation of a full STT-MRAM stack has been developed, using the Sentaurus commercial tool from Synopsis®. We have detailed the impact of the key parameters (the effective mass in barrier m_{ox}, the spin-splitting energy D_{spin} and the saturation magnetization M_S) in the Landau-Lifshitz-Gilbert equation on the simulated electrical I-V hysteresis loop at room temperature. The simulated realizations, including variability of the resistance values and of the switching voltages, are in very good agreement with experimental data. The thermal behavior of the two resistance values (R_P and R_{AP}) as well as the TMR ratio have also been simulated using the Sentaurus commercial tool. The simulation of the switching voltage dependence should still be performed, using the variation of the saturation magnetization of the ferromagnetic material M_S, using the Bloch law.

Acknowledgment

This work was supported by the grant n°ANR-19-CE39-0010 (MISTRAL Project) overseen by the French National Research Agency (ANR).

References

[1] M. H. Kryder and S. K. Chang, “After Hard Drives—What Comes Next?” IEEE Trans. on Magn., 45(10), 2009.

[2] A. Iyengar, S. Ghosh, N. Rathi, and H. Naeimi, “Side channel attacks on STTRAM and low-overhead countermeasures”, IEEE DFT, pp. 141-146, 2016.

[3] J. S. Moodera, Lisa R. Kinder, Terrilyn M. Wong, and R. Meservey, “Large magnetoresistance at room temperature in ferromagnetic thin film tunnel junctions”, Phys. Rev. Lett., 74, 1995.

[4] N. Yazigy et al., “Experimental analysis on stochastic behavior of preswitching time in STT-MRAM”, Micro. Reliab., 138, 2022.

[5] N. Yazigy et al., “Real-time electrical measurements during laser attack on STT-MRAM”, IEEE ICMTS, 2022.

[6] N. Yazigy et al., “Correlation between 1064 nm laser attack and thermal behavior in STT-MRAM”, Micro. Reliab., 150, 2023.

[7] F. O. Heinz and L. Smith, “Fast simulation of spin transfer torque devices in a general purpose TCAD device simulator”, IEEE SISPAD, pp. 127-130, 2013.

[8] T. L. Gilbert, “A Lagrangian formulation of the gyromagnetic equation of the magnetization field”, Physical Review, 100, 1955.

[9] T. Hadamek, S. Selberherr, W. Goes, and V. Sverdlov, “Modeling thermal effects in STT-MRAM”, Solid State Elec., 200, 2023.

[10] W. Guo et al, “SPICE modelling of magnetic tunnel junctions written by spin-transfer torque”, J. Phys. D: Appl. Phys., 43, 2010.

[11] S. Sampan-A-Pai et al., “Magnetization dynamics at finite temperature in CoFeB–MgO based MTJs”, Sci. Rep., 13, 2023.

[12] J. Chatterjee et al., “Physicochemical origin of improvement of magnetic and transport properties of STT-MRAM cells using tungsten on FeCoB storage layer”, Appl. Phys. Lett., 114(9), 2019.

[13] Sentaurus™ Device User Guide, Version M-2016.12, December 2016.

[14] Y. Zhang, “Edge Driven Magnetic Switching in CoFeB-MgO Based Spintronic Nanodevices”, PhD Thesis, Paris-Saclay University & Beihang University, 2018.

[15] H. Jang et al., “Thermal Conductivity of Oxide Tunnel Barriers in Magnetic Tunnel Junctions Measured by Ultrafast Thermoreflectance and Magneto-Optic Kerr Effect Thermometry”, Phys. Rev. Applied, 13 (2), 024007, 2020.

[16] A. Okada et al., “Magnetization dynamics and its scattering mechanism in thin CoFeB films with interfacial anisotropy”, Proc. Natl. Acad. Sci. USA, 114 (15), pp. 3815-3820, 2017.

[17] J. García-Otero, A. J. García-Bastida, and J. Rivas, “Influence of temperature on the coercive field of non-interacting fine magnetic particles”, J. of Magnetism and Magnetic Mat., 189 (3), pp. 377-383, 2020.

[18] Y. Takeuchi, H. Sato, , S. Fukami, F. Matsukura, and H. Ohno, “Temperature dependence of energy barrier in CoFeB-MgO magnetic tunnel junctions with perpendicular easy axis”, Appl. Phys. Lett., 107 (15), 152405, 2015.

[19] K.-M. Lee, J. W. Choi, J. Sok, and B.-C. Min, “Temperature dependence of the interfacial magnetic anisotropy in W/CoFeB/MgO”, AIP Advances, 7, 065107, 2017.

[20] Q. Hao and G. Xiao, “ Giant spin Hall effect and magnetotransport in a Ta/CoFeB/MgO layered structure: A temperature dependence study”, Phys. Rev. B, 91 (22), 224413, 2015.

[21] A. Deka et al., “ Electric-field control of interfacial in-plane magnetic anisotropy in CoFeB/MgO junctions”, Phys. Rev. B, 101, 174405, 2020.

[22] E. C. I. Enobio, M. Bersweiler, H. Sato, S. Fukami, and H. Ohno, “Evaluation of energy barrier of CoFeB/MgO magnetic tunnel junctions with perpendicular easy axis using retention time measurement”, Jpn. J. Appl. Phys., 57 (4S), 04FN08, 2018.

[23] A. Meo, R. Chepulskyy, D. Apalkov, R. W. Chantrell, and R. F. L. Evans, “Atomistic investigation of the temperature and size dependence of the energy barrier of CoFeB/MgO nanodots”, J. Appl. Phys., 128, 073905, 2020.

[24] V. Gopal, “Temperature Dependence of Effective Mass of Electrons & Holes and Intrinsic Concentration in Silicon”, Indian Journal of Pure & Applied Physics, 20, pp. 180-182, 1982.

[25] L. He and C. Chen, “Effect of temperature-dependent shape anisotropy on coercivity with aligned Stoner-Wohlfarth soft ferromagnets”, Phys. Rev. B, 75, 184424, 2007.